Prepared for the National Institutes of Health
National Institute of Neurological Disorders and Stroke
Division of Stroke, Trauma and Neurodegenerative Disorders
Neural Prosthesis Program
Bethesda, MD 20892

# Microstimulation of the Lumbosacral Spinal Cord: Mapping

## NIH-NINDS-NO1-NS-8-2300

## Quarterly Progress Report #2

Period Covered: 1 January, 1999 - 31 March, 1999

Principal Investigator: Warren M. Grill, Ph.D.

Co-Investigators: Musa A. Haxiu, M.D., Ph.D.
Michel A. Lemay, Ph.D.

Department of Biomedical Engineering
Case Western Reserve University
Cleveland, OH 44106-4912

## ABSTRACT

The objectives of this research are to determine the anatomical locations of spinal neurons involved in control of the genitourinary and hindlimb motor systems, and to determine the physiological responses evoked in the genitourinary and hindlimb motor systems by intraspinal microstimulation. During this quarter we made progress toward both of these objectives. We continued a series of experiments to characterize the hindlimb motor responses evoked by microstimulation of the lumbar spinal cord. The results demonstrate that endpoint force fields are of 4 primary types, and that there is a distinct difference in the patterns endpoint forces evoked directly by stimulation of motoneurons and endpoint force fields evoked indirectly by stimulation of more dorsal regions of the spinal cord. We also began work on an electrical technique to localize neurons in the spinal cord using recordings of electrical potential on the surface of the spinal cord. During this quarter we implemented a Fourier-based solution of Poisson's equation and replicated results for a point current source in a homogeneous medium.

## INTRODUCTION

Electrical stimulation of the nervous system is a means to restore function to individuals with neurological disorders. The objective of this project is to investigate the feasibility of neural prosthetics based on microstimulation of the spinal cord with penetrating electrodes. Specifically, chemical and viral retrograde tracers, immediate early gene expression, and immunocytochemistry are used to determine the locations and neurochemical content of neurons in the spinal cord that control genitourinary and motor functions in the male cat. Microstimulation with penetrating activated iridium microelectrodes to determine the physiological effects in the genitourinary and motor systems of activation of different neural populations. The results of this project will provide data important to understanding neural control of genitourinary and motor functions, answer fundamental questions about microstimulation of the spinal cord, and lead to development of a new generation of neural prosthetics for individuals with neurological impairments.

## PROGRESS IN THIS QUARTER

During the second quarter of this contract we continued a series of experiments to measure the endpoint force produced at the hindlimb by microstimulation of the lumbar spinal cord. We also began work on an electrical technique to localize neuronal populations within the spinal cord. We also constructed a d.c. constant current source for use in making tissue lesions to identify precisely the position of metal microelectrodes within the tissue. Below each of our accomplishments is summarized.

## Hindlimb Motor Responses Evoked by Intraspinal Microstimulation

Our previous high-resolution mapping experiments of single joint motor responses identified region of the lumbar spinal cord that produced hindlimb activation. The results demonstrated that maps were repeatable across experiments and that maps of motor responses generated by microstimulation in the ventral horn were in strong agreement with the known location of the motoneurons innervating the knee flexors and extensors. Further, dorsal stimulation produced ipsilateral flexion and contralateral extension- these responses were reminiscent of two classical spinal reflexes- flexion withdrawal and crossed extension.

More recently we have begun a series of experiments to further characterize the hindlimb motor responses evoked by microstimulation. In these experiments rather than recording single joint responses, we are recording the net force at the endpoint of the hindlimb. During the period covered by this quarterly progress report, we studied the spinal mapping of motor responses evoked by microstimulation of the lumber enlargement

## METHODS

The endpoint forces evoked at the paw by microstimulation of the lumbar spinal cord were recorded in anesthetized cats. All animal care and experimental procedures were according to NIH guidelines and were approved by the Institutional Animal Care and Use Committee of Case Western Reserve University.

### Experimental Preparation

Animals were anesthetized with ketamine HCl (Ketaset, 15-30 mg/kg, IM), a venous catheter was inserted in the cephalic vein, and anesthesia maintained with alpha-chloralose (Sigma, 60 mg/kg IV, supplemented at 15 mg/kg). A laminectomy was made to expose the lumbosacral spinal cord. The animal was mounted in a frame with pins at the hips, the head in a headholder, and vertebral clamps at L3 and S1. The femur was fixed with a steel pin, and the paw was attached to a gimball mounted on a 3-axis force/moment transducer (Nano-17, ATI Inc., Garner, NC). The force transducer was mounted on a cartesian manipulator that allowed positioning of the force sensor throughout the workspace of the lower leg and paw, while the gimball permits the rotation of the ankle when the limb is moved. Fine bifilar wire electrodes were inserted into four hindlimb muscles (knee flexor, knee extensor, ankle flexor, and extensor) to record the electromyographic (EMG) activity. Body temperature was maintained between 37° and 39° C with a thermostatically controlled heat lamp, 0.9% saline with 8.4 mg/cc sodium bicarbonate and 5% dextrose added was administered IV (~20 cc/hr), respiration was maintained with a respirator, and electrocardiogram was monitored throughout the experiment. Dexamethasone (2 mg/kg) was administered at the completion of the laminectomy and every 6 hours thereafter for the duration of the experiment.

The dura was opened, the levels identified by root exit, the spinal cord was covered with warm mineral oil, and microstimulation commenced. Vertical, dorsal-to-ventral penetrations were made to position electrodes at locations identified in our previous high-resolution mapping studies to evoke hindlimb motor responses. Activated iridium wire microelectrodes (50 μm diameter) with an exposed electrochemically determined surface area of ~225 $\mu m^2$, a 1-3 μm tip, and insulated with Epoxylite were

used (IS300, Huntington Medical Research Institutes, Pasadena, CA). Stimuli were charge balanced biphasic pulses with a cathodic phase amplitude of 10-100 μA and duration of 100 μs applied at 40 Hz for 0.5 s. The amplitude of the anodic phase was limited to 100 μA and the duration was set automatically by the stimulator to balance the charge in the primary phase.

At selected depths for each of the penetration the limb was moved on a 3cm grid of nine to twelve points from a mid-stance position while stimulation parameters and electrode position are kept constant. The forces measured at those nine to twelve locations were used to calculate the forces acting on the limb's end-point throughout the workspace. The workspace was divided into triangles, and the forces within a triangle were estimated by a linear interpolation based on the three vectors measured on the vertices (see Fig. 2.1). Note that although we measured forces and moments along three orthogonal axes (x, y and z) our analysis is limited to the sagittal plane. Furthermore, the forces were divided into a passive component (force measured before the onset of activation), and an active component (total forces measured minus the passive portion). Total, active and passive force fields were reconstructed. The forces due to gravity were calculated using simple mechanics and subtracted out. The calculation of the ankle and knee moments due to gravity requires the distance from the proximal joint to center of mass of leg and paw. Those parameters were obtained using equations that calculate those parameters as a function of the cat's weight, and segments' lengths [Hoy and Zernicke, 1985].

The torques acting at the knee and ankle joints are calculated from the force measurements and are given by $\mathbf{T}=\mathbf{J}^{T}\mathbf{F}$, where $\mathbf{T}$ is the torque vector (knee, and ankle), $\mathbf{F}$ is the force vector (Fx, and Fy), and $\mathbf{J}^{T}$ is the transpose of the limb's Jacobian. Calculating the Jacobian requires the link lengths (obtained via post-mortem X-rays of the animal), and joint angles (calculated using link lengths measurements, and the position of the knee joint relative to the force sensor transport mechanism origin).

The electromyographic (EMG) activity of four hindlimb muscles was measured simultaneously with the evoked forces. EMG was measured from *biceps femoris*, *vastus*, *tibialis anterior*, and *medial gastrocnemius*, and electrode location was verified via post-mortem dissection. The raw EMG signals were amplified, filtered (10-1000Hz), and sampled at 2500Hz.

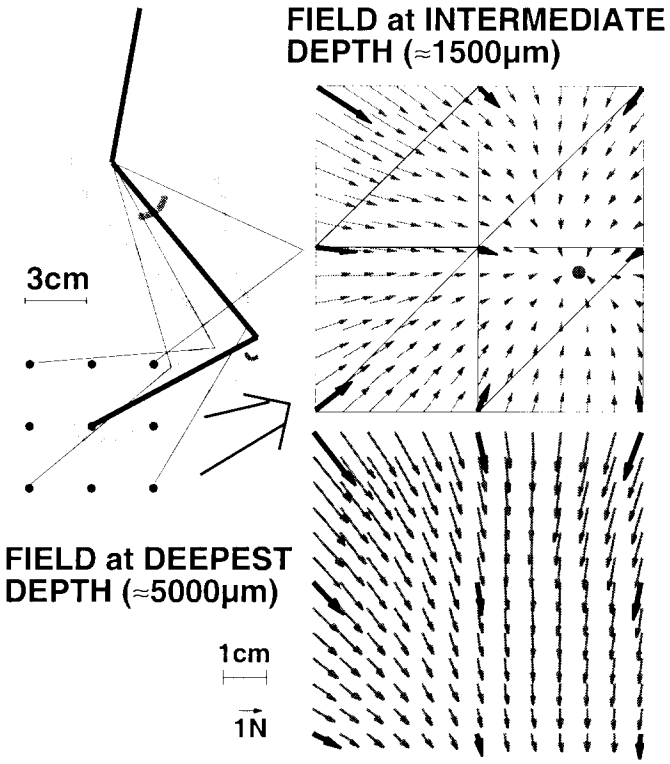


**Figure 2.1** Force field construction. Left top: spatial locations where forces are recorded. With the femur held fixed via pins, the knee and ankle are moved through a large range-of-motion (walking range-of-motion shown as thick arc-circles). Right top: actual force vectors measured (thick dark vectors), triangles dividing the workspace, and the interpolated force vectors (thin light vectors). Forces represented are the total forces (active and passive) minus the gravity component. The top right field exhibited convergence, i.e. the net end-point forces go to zero at a location in the workspace, while the bottom field obtained at greater depth did not.

## RESULTS

The passive force fields (i.e., no stimulation) measured in two animals (SFF02 & SFF03) were very similar (Fig. 2.2). Both fields show increasing extension forces as the leg was flexed, and decreasing extension forces as the leg was extended. In the rostrocaudal direction, both fields tended to restore the limb towards the middle. In these examples, the leg was not sufficiently extended to show the expected reversal from extension forces to flexion forces as the limb reached the extension limits.

Active force fields were of four primary types (Fig. 2.3): flexion withdrawal, rostral flexion, caudal extension, and rostral extension. Flexion withdrawals were the most common field encountered, especially at superficial depths of penetration (≈800 μm). The force responses of flexion withdrawal fields accommodated quickly (≈250 ms). These responses were likely the result of activation of afferent fibers/terminals. However, similar fields are evoked by stimulating in the same area in chronically spinalized and deafferented rats [Tresch, 1997], and therefore we cannot rule out the hypothesis that flexion withdrawal fields were due to activation of interneurons. Extensor fields were most commonly encountered at greater depths (≈ 5000μm), and appeared to

be the result of direct activation of motoneurons. Fields found at intermediate depths (≈1500μm) presented the greatest variety of structure.

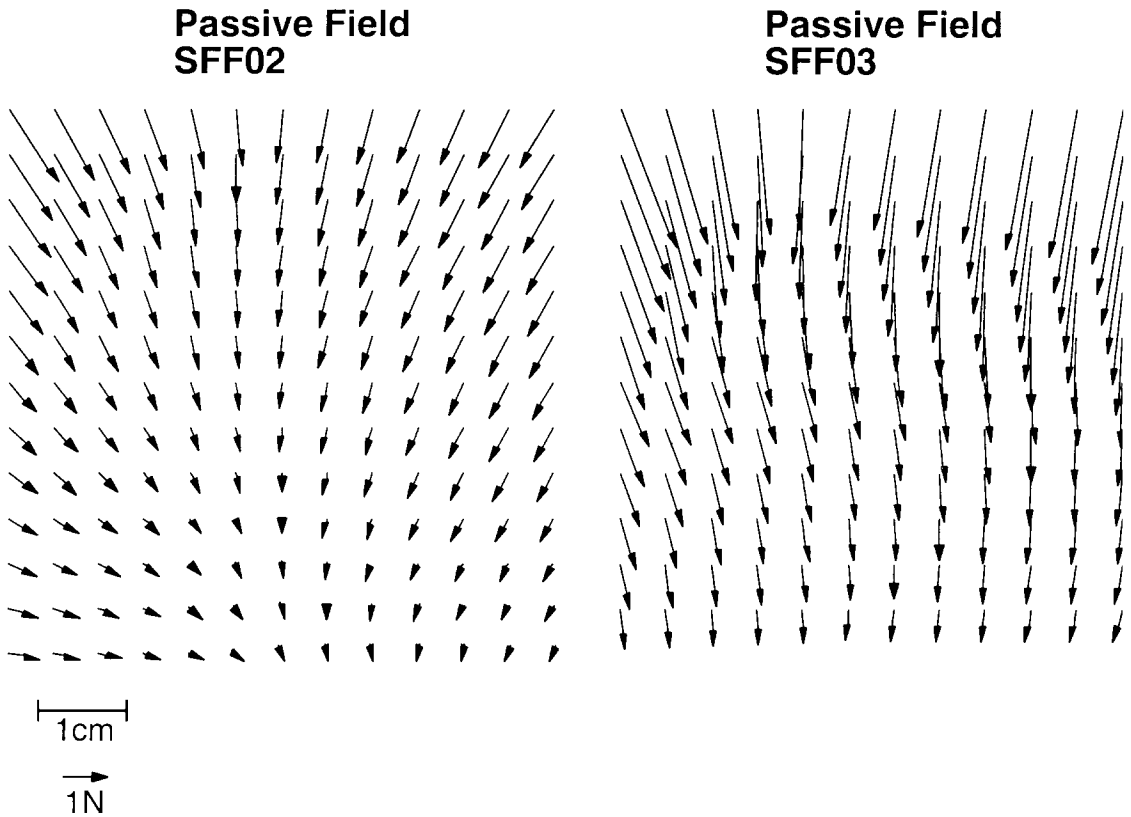


**Figure 2.2** Passive force fields (without gravity) for two animals (SFF02 and SFF03).

The characteristics of force fields differed between ventral *versus* dorsal and intermediate locations. Endpoint forces evoked by stimulation at dorsal or intermediate locations varied both in direction and magnitude with the limb's configuration. For some stimulation sites, the endpoint forces varied so as to produce a force pattern which converged to a point in the workspace where the net endpoint force was zero (Fig. 2.1). The EMG activity of the four hindlimb muscles monitored indicated that the convergent fields were produced by co-activation of multiple muscles. In contrast, while the magnitude of endpoint forces evoked by ventral microstimulation varied with limb position, their directions were largely invariant, and the resulting fields were parallel or divergent (see Fig. 2.1, and Fig. 2.3 C and D). Similar patterns were evoked by intramuscular stimulation of single muscles as shown in Figure 2.4.

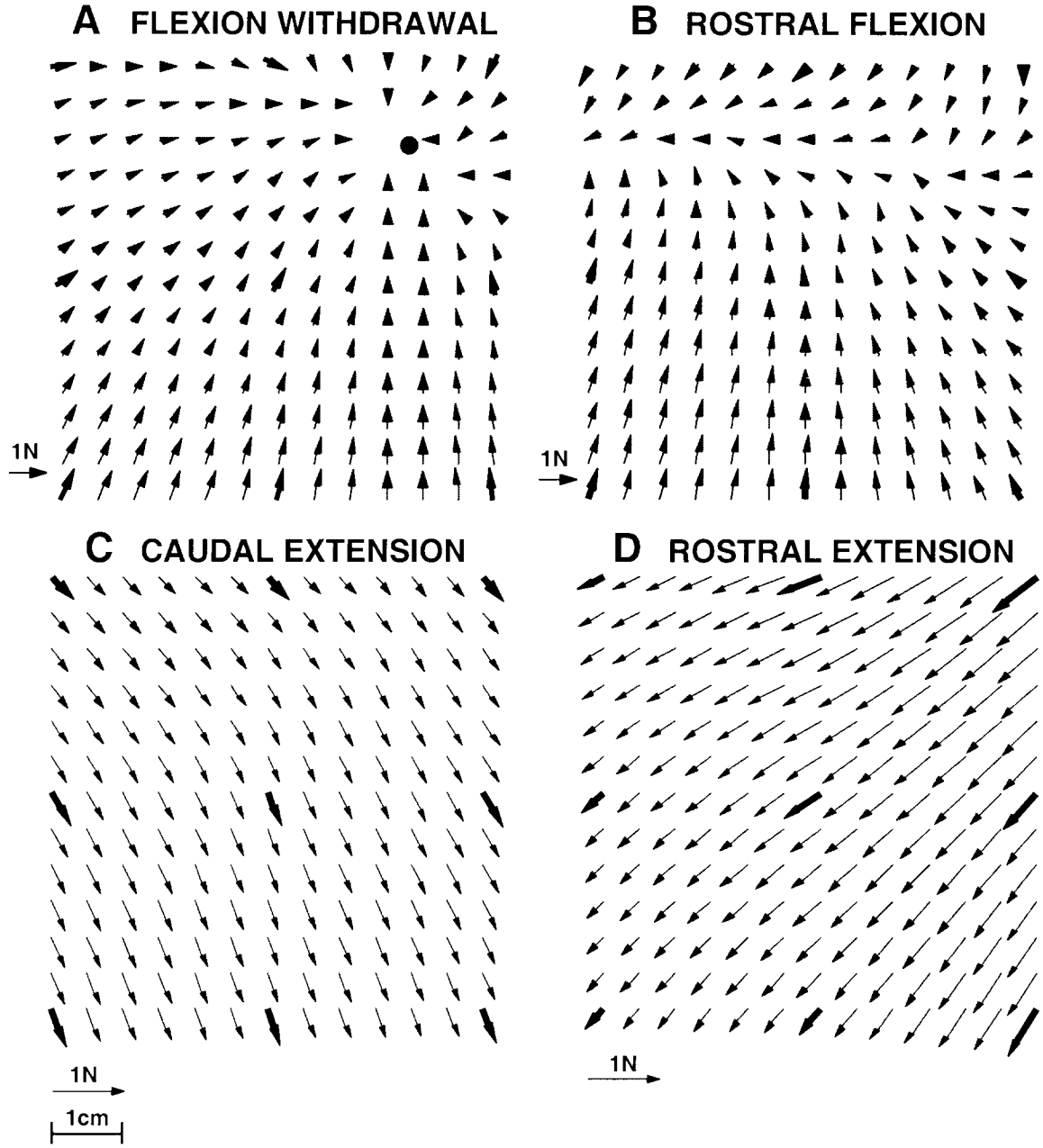


**Figure 2.3** The four active force field types. A Flexion withdrawal (depth 3400μm), B Caudal flexion (depth 3400μm) C Rostral extension (depth 4600μm), and D Caudal extension (depth 5000μm).

Of the 33 fields measured over 17 penetrations in two animals, 58% were flexor withdrawal, 36% were caudal extension, and 6% were rostral extension. No rostral flexion was found in these two animals. The spinal cord region covered extended from 1 mm rostral to the L6/L7 border to 0.4 mm caudal to the border, and from 1550 μm contralateral to the midline to 2100 μm ipsilateral to the midline. None of the active force fields presented a point of convergence within the workspace (unlike in the first experiment reported in QPR 1). Of the 33 total (active + passive) force fields, 27% presented a point of convergence within the workspace.

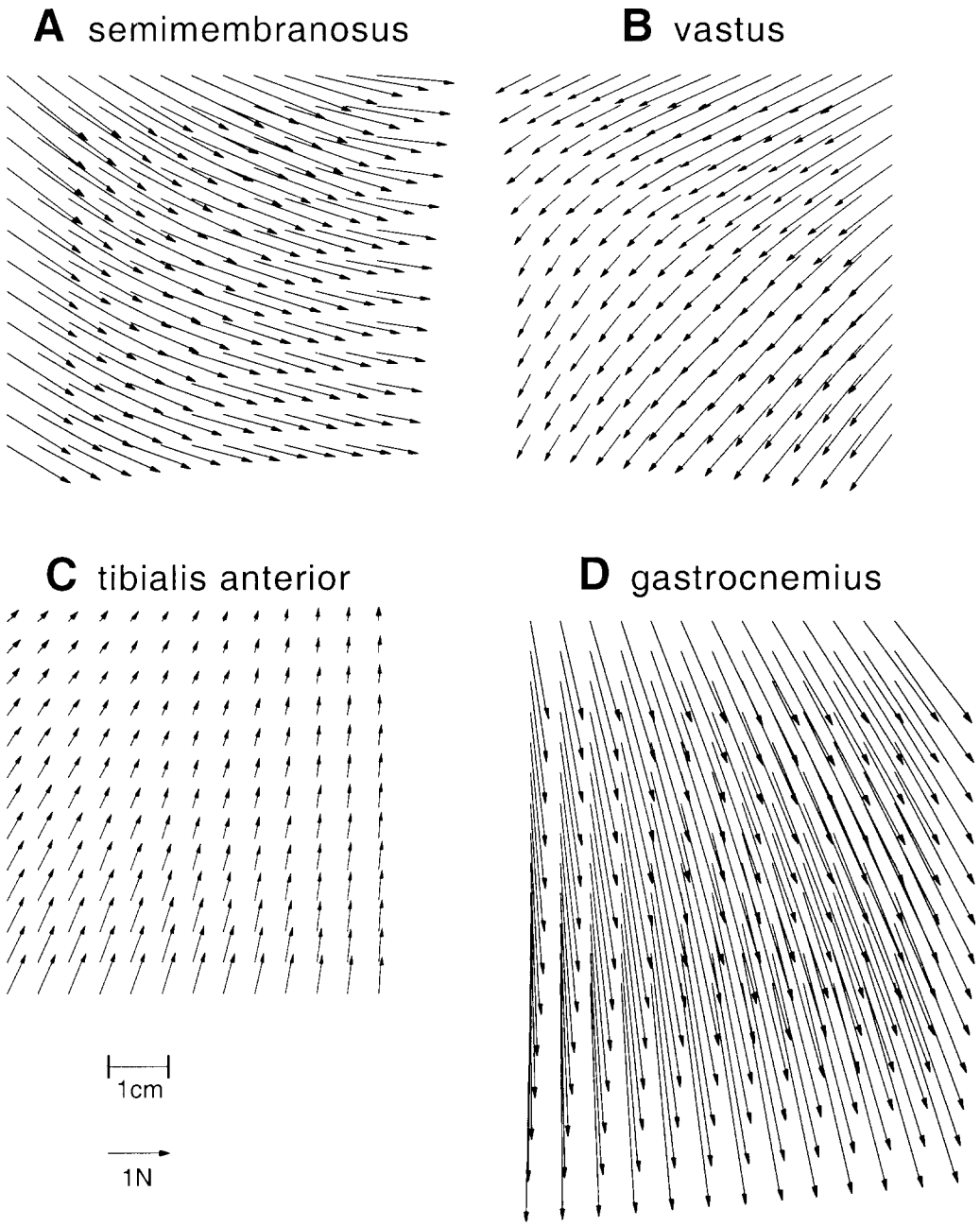


**Figure 2.4** Force field produced via activation of a single muscle: A *tibialis anterior*, B *medial gastrocnemius*, C *semimembranosus*, and D *vastus*. These fields were similar to the fields evoked at greater depth of penetration (see Fig. 1, and Fig. 3 C and D), and showed no convergence.

## CONCLUSIONS

Our measurements of endpoint forces in anesthetized, spinal-intact cats indicate that stimulation in the dorsal and intermediate aspects of the spinal cord generate organized, convergent force patterns. Our results were obtained in spinally intact animals, but previous data from spinal rats indicate that these patterns are preserved following spinal injury [Tresch, 1997].

These results suggest that microstimulation of the mammalian spinal cord can be used to activate groups of muscles to produce organized force patterns at the limb's endpoint. This finding may find application in neural prosthetic control of multi-joint movement in persons with spinal cord injury.

**Source Localization for Electrical Mapping of Spinal Neurons**

The objective of this project is to develop an intraoperative mapping technique to identify the location of the neurons targeted for stimulation.. We have previously developed techniques for spinal cord mapping in animal models using electrical stimulation as well as immediate early gene expression [Grill et al., 1998]. However, less invasive methods are required for in vivo mapping.

Therefore, we are undertaking to develop a solution of the inverse problem: given the potentials on the surface of the spinal cord, reconstruct the location of the source that produced those potentials [Oostendorp and Van Oosterom, 1989]. As a first step in developing this technique, we are using computer modeling to assess the feasibility of our proposed approach.

**METHODS**

We have implemented in MATLAB a Fourier-based method for solution of the potentials generated by current sources in cylindrical volume conductors. The Fourier method allows the calculation of a two-dimensional array of potentials in the frequency domain, and the solution in the space domain is obtained using a fast Fourier transform algorithm. Thus, the Fourier method allows operation on an array of points in space, instead of solving for each point separately.

**RESULTS**

To verify our algorithm, we have implemented a solution of the potentials produced by a current source in an infinite homogenous isotropic conductive medium. The method can solve the point source problem for an array of 16,384 points (512 x 32) in less than one minute; solving the problem in cylindrical coordinates without the Fourier method would take a time approximately four orders of magnitude longer. The frequency array and the space domain solution shown in fig. 2.5 match previously published results obtained using the Fourier method [Altman and Plonsey, 1988].

The Fourier solution was also compared with the analytical solution ($V=I/(4\pi\sigma R)$ as shown in fig. 2.6. The slight difference between the lines results from the discretization error associated with the Fourier technique and can be eliminated by decreasing the sampling interval.

These results demonstrate the efficiency and accuracy of the Fourier-based method that was implemented during this quarter.

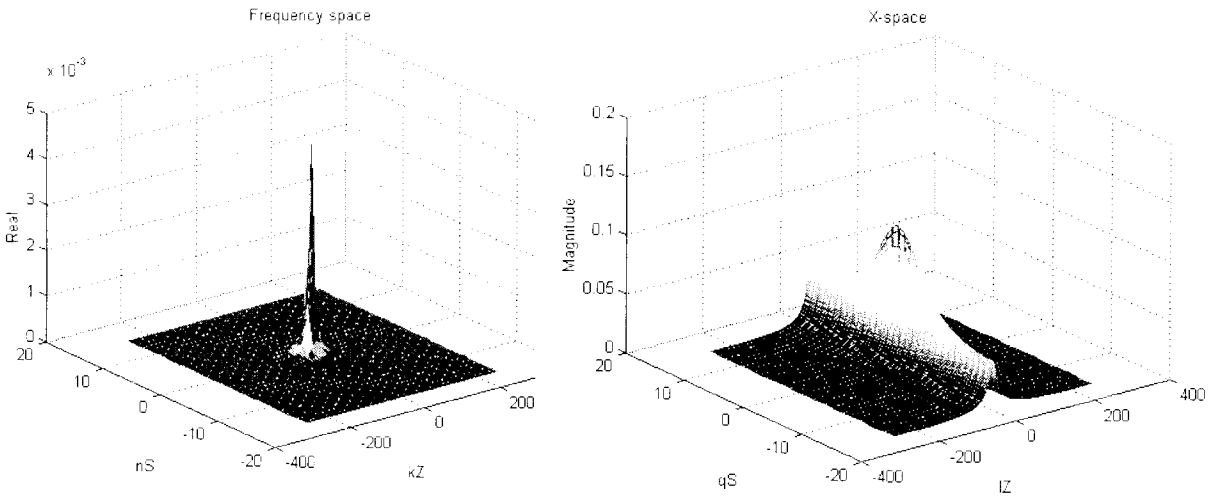


**Figure 2.5** Potentials produced by a point current source in an infinite isotropic medium solved using a Fourier transform technique. The solution to Poisson's equation is obtained in the frequency domain (left plot shows the potential as a function of the azimuthal {nS} and longitudinal {kZ} frequency), and the inverse Fourier transform is used to obtain the potentials space domain (right plot shows the potential as a function of the azimuthal {qS} and longitudinal {lZ} positions).

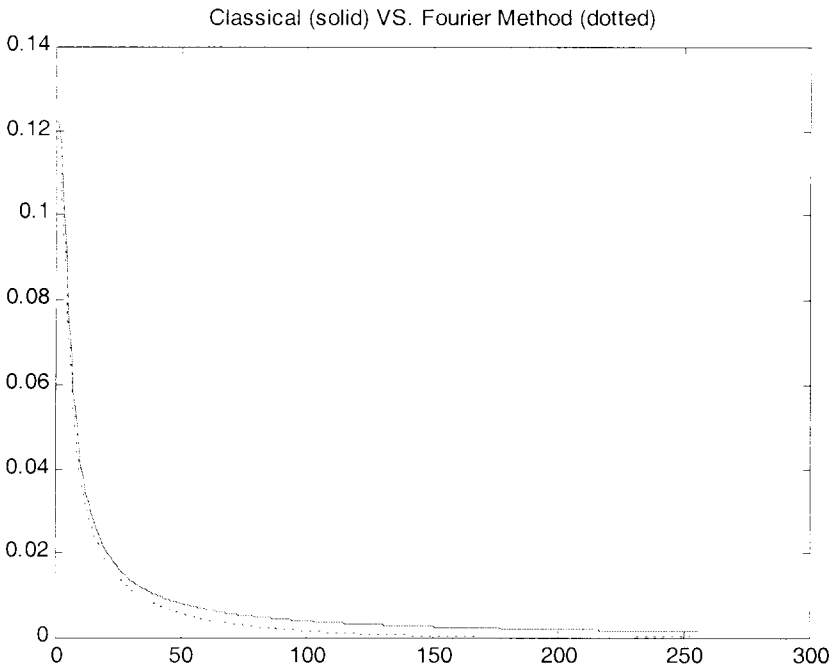


**Figure 2.6** Potential as a function of position for a point current source in a homogeneous isotropic medium solved using an analytical or Fourier method.

## Fabrication of a d.c. Regulated Current Generator

Although use of d.c. currents is an established technique to make either metal deposition or tissue lesions, parameters for use with activated iridium microwire electrodes have not been determined. Therefore we designed and constructed a versatile d.c. constant current source to use in establishing parameters for creating small spinal cord lesions with activated iridium microwire electrodes (fig. 2.7).

The specifications for the device called for a time controlled adjustable current from 0-100 uA across impedances up to 1 MΩ. The timing of the circuit was done using an ICM7250 timing chip and was designed to provide 0 to 99 seconds in one second increments of DC current. To generate sufficient current across a large load, a minimum of 100 V was required across the load. This voltage was generated from a 9 V lithium-ion battery using a Maxim 773 DC-DC converter. The high voltage required the use of a special high-voltage operational amplifier, Apex Microtechnology PA81J. The operational amplifier was configured as a modified Howland current pump with a floating load. Current pulse duration is set with a thumbwheel and current amplitude is controlled using a 10 turn precision potentiometer. A 1 kΩ resistor in series with the load enables the user to monitor the current output using an oscilloscope or voltmeter. This device was fabricated and operates within specifications under bench testing.

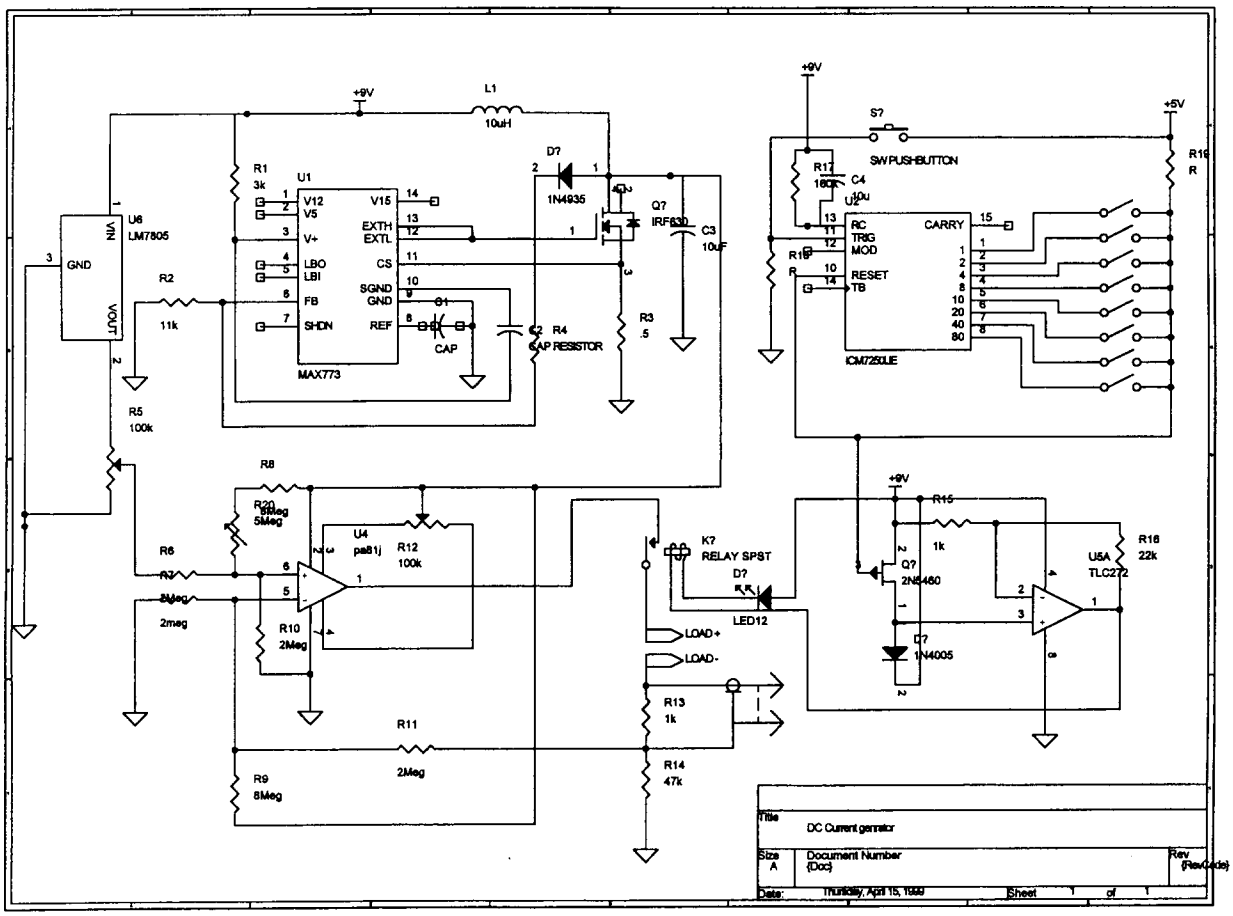


**Figure 2.7** Circuit diagram of the d.c. regulated current source.

## PUBLICATIONS THIS QUARTER

Wang, B., N. Bhadra, W.M. Grill (1999) Functional anatomy of the male feline urethra: morphological and physiological correlations. J. of Urology 161:654-659.

McIntyre, C.C., W.M. Grill (1999) Excitation of central nervous system neurons by non-uniform electric fields. Biophysical Journal 76:878-888.

Lemay, M.A., W.M. Grill (1999) Endpoint forces evoked by microstimulation of the cat spinal cord. submitted to the 21st Annual Int. Conference of the IEEE-Engineering in Medicine and Biology Society.

Lemay, M.A., W.M. Grill (1999) Spinal force fields in the cat spinal cord. Submitted to the 25th Annual Meeting of the Society for Neuroscience.

## OBJECTIVES FOR THE NEXT QUARTER

In the next quarter we will continue our co-localization studies to identify inhibitory spinal neurons active during micturition. Our specific objectives are to complete quantification of results co-localizing c-Fos with parvalbumin and c-Fos with GABA, and to prepare a manuscript reporting these results. We will also continue our studies characterizing the hindlimb motor responses to lumbar microstimulation. Our specific objective is to investigate the spinal motor responses in decerebrated preparations. Our hypothesis is that the heightened reflexive state will uncover responses that are currently suppressed by anesthesia. Finally, we will continue development of our electrical mapping method. Our specific objective is to implement the electrical field solution for a dipolar source in a cylindrical volume conductor, solved using the Fourier method implemented during the current quarter.

## LITERATURE CITED


Altman, K.W., R. Plonsey (1988) Development of a model for point source electrical fiber bundle stimulation. Med. Biol. Eng. Comput. 26:466-475.

Giszter, S.F., F.A. Mussa-Ivaldi, E. Bizzi (1993) Convergent force fields organized in the frog's spinal cord. J. Neuroscience 13:467-491.

Grill, W.M., B. Wang, S. Hadziefendic, M.A. Haxhiu (1998a) Identification of the spinal neural network involved in coordination of micturition in the male cat. Brain Research 796:150-160.

Hoy, MG and RF Zernicke. "Modulation of limb dynamics in the swing phase of locomotion." J Biomech. 18(1 1985): 49-60.

Oostendorp, T.F., A. Van Oosterom (1989) Source parameter estimation in inhomogeneous volume conductors of arbitrary shape. IEEE Trans. Biomed. Eng. 36:382-391.

Tresch, MC. "Discreteness in spinal motor systems in the rat and frog." Ph.D. Dissertation, Massachusetts Institute of Technology, Cambridge, MA, 1997.